Growth and properties of self-assembled monolayers on metals

Article *in* Journal of Physics Conference Series · April 2009

DOI: 10.1088/1742-6596/152/1/012029

3 authors, including:

Yanxin Zhuang
Northeastern University (Shenyang, China)
60 PUBLICATIONS **864** CITATIONS

SEE PROFILE

Growth and properties of self-assembled monolayers on metals

2009 J. Phys.: Conf. Ser. 152 012029

(http://iopscience.iop.org/1742-6596/152/1/012029)

Journal of Physics: Conference Series **152** (2009) 012029 doi:10.1088/1742-6596/152/1/012029

Growth and properties of self-assembled monolayers on metals

Y X Zhuang[1, 2], O Hansen[2] and J C He[1]

[1]Key laboratory of Electromagnetic Processing of Materials, Ministry of Education, Northeastern University, Shenyang, 110004, P.R. China
[2] Department of Micro- and Nanotechnology, DTU Nanotech and CINF, Technical University of Denmark, Building 345 east, DK-2800, Kgs. Lyngby, Denmark

[1]Email: yxzhuang@epm.neu.edu.cn

Abstract. Self-assembled monolayers (SAMs) grown from organosilane are promising candidate for anti-stiction coatings. It is well know that the application of hydrocarbon- and fluorocarbon-based SAMs can significantly reduce stiction and adhesion in silicon micro/nanostructures in Micro-Electro-Mechancial System (MEMS). There are often various metals involved in MEMS, such as Au, Al, Ti, etc. In the process of growing anti-stiction SAMs on the silicon microstructures, SAM will be unavoidably deposited on the metals, which will significantly change surface properties of the materials. Therefore, it is necessary to investigate how the organosilane SAMs grow on the metals, and affect the surface properties of the materials. In this paper, $CF_3(CF_2)_5(CH_2)_2SiCl_3$ (FOTS) SAMs were grown on various metals using a vapour phase process in a home-made setup. The metals investigated are thin film Pd, Au, Ni, Al, Ti, Cr with thickness of 100 nm, which are deposited on monocrystal-silicon substrates using e-beam evaporation. The SAMs were characterized by static contact angle, surface energy, roughness, nano-scale adhesion force and friction force.

1. Introduction

Self-assembled monolayer (SAM) coatings have attracted considerable scientific and industrial interest due to their good bonding strength, low surface energy, low friction forces, and good thermal stability [1-6]. Applications range from functionalization of surfaces for bio-technology application to control of adhesion, friction and wear in microdevices and in Nanoimprint Lithography (NIL). Self-assembled monolayers (SAMs) can be deposited either in a liquid phase process or in a vapor phase process. Liquid phase deposition of SAM coatings has significant disadvantages, such as complicated process control, generation of large amounts of contaminated effluents, insufficient stiction prevention and high production costs. Vapor phase SAM deposition can eliminate some drawbacks of liquid-based SAM deposition, and thereby attract strong attention [7-8].

It is well know that the application of hydrocarbon- and fluorocarbon-based SAMs can significantly reduce stiction and adhesion in silicon micro/nanostructures. Meanwhile, there are often various metals involved in MicroElectroMechanical System (MEMS), such as Au, Al, Ti, Pt, Ni, etc. In the process of growing anti-stiction self-assembled monolayers on the silicon microstructures, SAMs will be unavoidably deposited on the metals. This significantly changes surface properties of the materials. Therefore, it was decided to investigate the growth and properties of organosilane SAMs on the metals. A self-assembled monolayer was deposited onto the various metal surfaces using the

same process as that used for silicon microstructures. The water contact angles, surface energy, nanoscale adhesion force and friction force of the SAM coatings were characterized.

2. Experimental techniques

The metals investigated are Au, Ni, Al, Pd, Cr, and Ti. The various metals with the thickness of 100 nm were deposited onto monocrystal silicon substrates using e-beam evaporation, where a 10 nm Ti layer was used as an adhesion layer for the deposition of Au, Ni, Al and Pd. The wafers with metal and monocrystal silicon (as a reference) were produced using the processes of photolithography, metal deposition, and lift-off. Afterwards, self-assembled monolayers were grown on silicon and various metals using a vapor phase process with $CF_3(CF_2)_5(CH_2)_2SiCl_3$ (FOTS) as a precursor. The vapor phase coating process was carried out in a home-made setup, which comprises a chamber, precursor injection system, vacuum system etc. Before the actual coating process, an O_2-plasma pretreatment step was applied in order to terminate the wafer surface with -OH groups. The substrates were left in the air (clean-room environment) for 3-4 hours to get enough water adsorbed on the surfaces, and then were loaded into the chamber. After pumping down the system, a certain amount (around 25 μL) FOTS was injected into the system, and kept 15 minutes for reaction. Then, the reaction chamber was pumped down and vented to take out the samples with FOTS self-assembled monolayers.

The contact angle measurements were performed using a contact angle meter DSA10 from Krüss GmbH equipped with an automatic dispensing system for four liquids and a frame grabber. Static contact angles were used to evaluate the SAM coatings. The static contact angle values were taken 5 seconds after deposition of the droplets on the surface to allow droplets relaxation. At least ten measurements were performed for each droplet. The static contact angle values reported in the work are the average value of measurements on at least ten droplets. The surface energy of coatings was calculated from static contact angles of deionised water and diiodomethane according to the Owens–Wendt–Rabel–Kaelble method, as described in ref [9].

The microtopography and roughness of the FOTS coatings were investigated using a commercial AFM system (NanoMan, Digital Instrument, Santa Barbara, CA, USA) in tapping mode with commercial silicon tips. The images were analyzed using the software Nanoscope 6.13 (Digital Instrument, Santa Barbara, CA, USA). The average roughness R_a, root-mean-square roughness RMS, and maximum peak roughness R_{max} were extracted from the images. All roughness data were obtained from a 2×2 μm^2 scanning area in order to eliminate the scanning length effect. AFM observations were performed at different positions to characterize the coating homogeneity.

Nanoscale adhesion and friction force measurements were carried out using a commercial AFM system (NanoMan, Digital Instrument, Santa Barbara, CA, USA) that is operated under ambient conditions at 22^{o}C and 45%–55% relative humidity. Square pyramidal Si_3N_4 tips with a nominal tip radius in the range of 20–60 nm that were mounted on gold-coated Si_3N_4 cantilevers with a nominal spring constant of 0.12 N/m (Digital Instrument, Santa Barbara, CA) were used in this work. The real spring constant of the AFM cantilever used in this work was 0.07 N/m which was determined using "cantilever on cantilever" method. The adhesion force measurements were carried out in the force calibration mode. The normal force calibration constant was obtained from the force-distance curve of the same AFM tip on a nature diamond [6]. For each sample, the adhesion forces were measured in more than 15 different locations. AFM friction measurements were done in lateral force microscopy mode. All scans were performed in a direction that is perpendicular to the long axis of the cantilever beam with a tip velocity of 4 μm/s and a scan length of 2 μm. For each sample, the friction tests were performed at at least three different locations. For easy comparison, all data presented in one plot were obtained with the same AFM tip. A detailed explanation of adhesion and friction measurement can be found in ref [6].

3. Results and Discussions

The static contact angles of water on the surfaces were measured at different process steps, such as after lift off, after O_2-plasma treatment, immediately after the FOTS deposition, and 2 weeks after the

FOTS deposition. Figure 1 gives the static water contact angle of the surfaces at each step. It can be seen that all the surfaces have similar wettability (water contact angle is around 80 degrees) after lift-off process. After 2 min O_2 plasma treatment, the water can completely spread on the silicon surface, indicating that the pre-treatment is good enough for growing FOTS self-assembled monolayer on silicon substrate. Even though the water contact angle on metal surfaces decreases after the oxygen plasma treatment, the wettability is not as good as that of silicon. After FOTS depositing on the surfaces, the water contact angle increases for all the surfaces. The water contact angles are larger than 110 degrees for freshly deposited FOTS on the Ti, Al, and Si substrates, indicating that the FOTS has high coverage and is well grown on those substrates. Meanwhile, the water contact angles remain same after 14 days. FOTS on other metals behave differently though. For example, the water static contact angles of freshly deposited FOTS on Au, Pd, and Ni substrates are only about 46, 84 and 62 degrees, respectively, suggesting that the FOTS coating has very poor coverage, and the FOTS molecules might be physically adsorbed onto those substrates. And the water contact angle increased after 14 days for the FOTS coatings on Au and Ni, which might be induced by contamination.

Figure 2 shows the AFM images of FOTS grown on the various metals and silicon. It should be mentioned that the z-scale used in the AFM images are different. The z-scale is 60 nm for FOTS on Au, Pd, Ni, Ti, and Al, 20 nm for FOTS on Cr, and 5 nm for the FOTS on Si, respectively. It can be seen that the roughness of FOTS on various metals is significantly larger than that of FOTS on monocrystal-silicon, which is caused by larger roughness of metal substrates. Meanwhile, there are aggregations observed on some silicon reference samples (not shown in this paper), which is due to larger amount of water adsorbed on the substrates before the sample being loaded into the reaction chamber. Figure 3 summarizes the RMS roughness, nano-scale adhesion force, and static contact angle of freshly deposited FOTS. The contact angles are strongly dependent on the surface energy of the surface materials and the topography of the surfaces. Larger roughness of Ti and Al explains that the water contact angle of FOTS on Ti and Al substrate is larger than that of FOTS on silicon. The surface energy of FOTS on Au, Pd, Ni, Al, Ti, Cr, and Si substrates (after 14 days storing) are 37.8, 26.2, 14.9, 10.2, 9.9, 11.5, and 11.2 mJ/m^2, respectively. The static water contact angle of freshly deposited FOTS on Cr, Si, Al and Ti are larger than 100^o, while the contact angles of other surfaces are less than 90^o. The roughness of FOTS on various metals is larger than that of silicon. It can be seen that FOTS on monocrystal silicon has largest nano-scale adhesion force even though it has higher static contact angle than others. It is well know that the nano-scale adhesion force is determined by the surface energy and the roughness of surfaces. The smaller the surface energy, the smaller the adhesion force is. The larger the roughness, the smaller the adhesion force is. This explains why FOTS on Au, Pd and Ni has smaller nano-scale adhesion force.

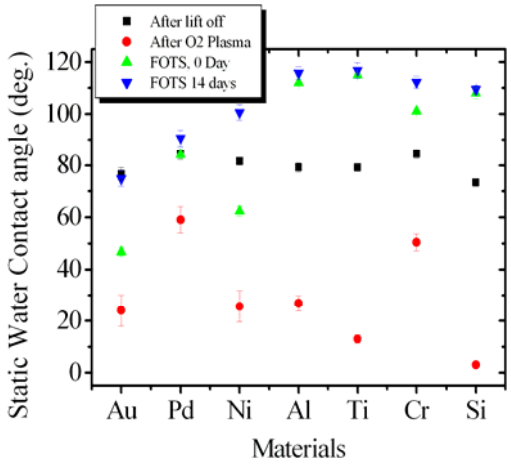

Figure 1. Static water contact angle of the various surfaces (Au, Pd, Ni, Al, Ti, Cr, and Si) measured after individual step, such as after lift off, after O_2 plasma pretreatment, on freshly deposited FOTS, and on FOTS 14 days after deposition.

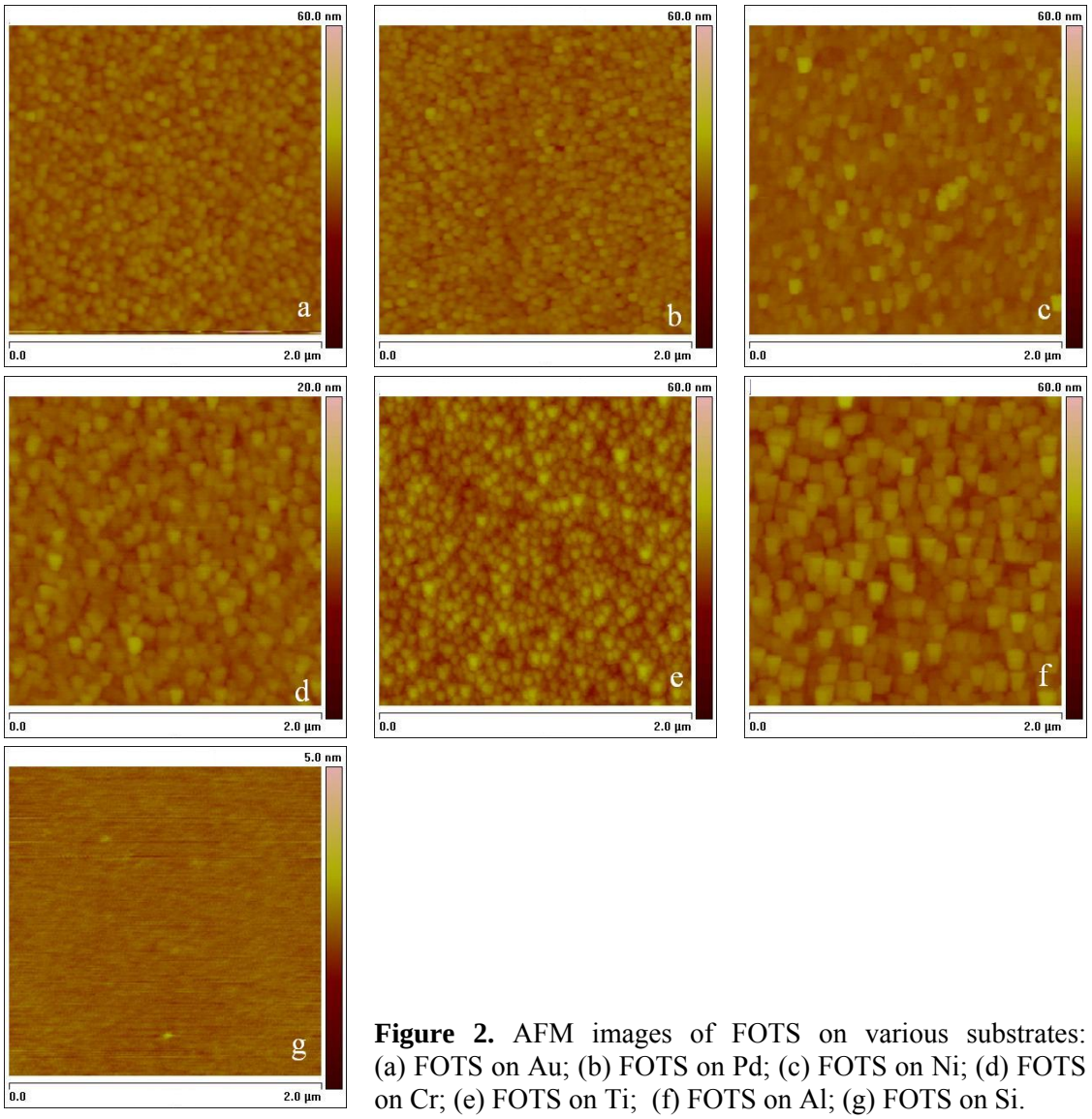

Figure 2. AFM images of FOTS on various substrates: (a) FOTS on Au; (b) FOTS on Pd; (c) FOTS on Ni; (d) FOTS on Cr; (e) FOTS on Ti; (f) FOTS on Al; (g) FOTS on Si.

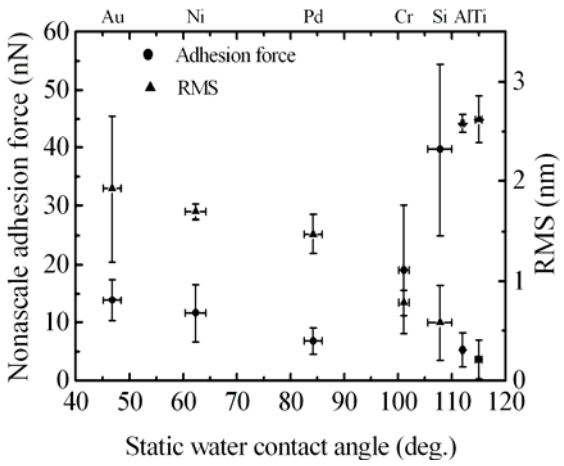

Figure 3. Nano-scale adhesion force, static water contact angle and roughness of FOTS on various metals and monocrystal-silicon.

Figure 4a gives variation of friction signal with normal load for FOTS on Si, Pd and Al. The FOTS coatings on other substrates have similar behavior. An approximately linear response is observed in the plot of friction signal versus normal load, suggesting that no substantial plastic deformation occurs in the testing range. Furthermore, the curve of FOTS on Pd is well above that of FOTS on Al and Si. The relative friction coefficient is defined as the slope of the friction signal versus normal load and is used as a parameter in comparing the friction behavior of FOTS on various substrates. It is well known that the following relationship exists between the friction force F and external normal load W [10]

$$F = \mu(W + W_a) \quad (1)$$

where μ is the friction coefficient and W_a is the adhesion force between the surface and AFM tip. Based on this equation and the data in Figure 4a, the μ and W_a values can be calculated. Figure 4b illustrates the relative friction coefficient of FOTS on various substrates, and the inset in Figure 4b shows the adhesion force determined from equation (1) and data in Figure 4a. It can be seen that the substrate can be considered as two groups. One group has larger static water contact angle, and low friction force, such as FOTS on Cr, Al, Ti and Si, which normally has a native oxide on the metal surface. The other group is Au, Pd, and Ni, which has smaller water contact angles and larger friction force. It has been suggested [10] that a chemical adsorbed self-assembled molecule on a surface can be regarded as an assembled molecular spring anchored to the surface. Therefore, a Si_3N_4 tip sliding on the surface of SAMs is similar to the tip sliding on the top of molecular springs or a molecular brush, which consists of a number of molecular springs. The monolayer can be elastically compressed under certain conditions, and the monolayer becomes disorder at the higher load. Based on these assumptions, a molecular spring model was proposed [10]. The molecular spring assembly has compliant features and can experience change in orientation and compression under normal load. The tilt angle of the molecules relative to the surfaces changes under the normal load applied by the AFM tip. The orientation of the "molecular springs or brush" under normal load reduces the shearing force at the interface, which in turn reduces the friction forces. In elasticity deformation range, when the tip slips away, the orientated and compressed molecules can recover to their initial state. The possibility of orientation is determined by the spring constant of a single molecule, as well as the interaction between the neighboring molecules, which is reflected by the packing density. The more molecules anchored on the unit surface, the higher coverage is, and the higher packing density is. The different friction forces of FOTS on various substrates can be explained by different coverage of the coatings (or packing density). The lower relative friction force of FOTS on Al, Cr, and Si might indicate that higher coverage of FOTS on those surfaces. However, it can not explain why the FOTS on Ti has larger friction force. The reason for that is still unknown.

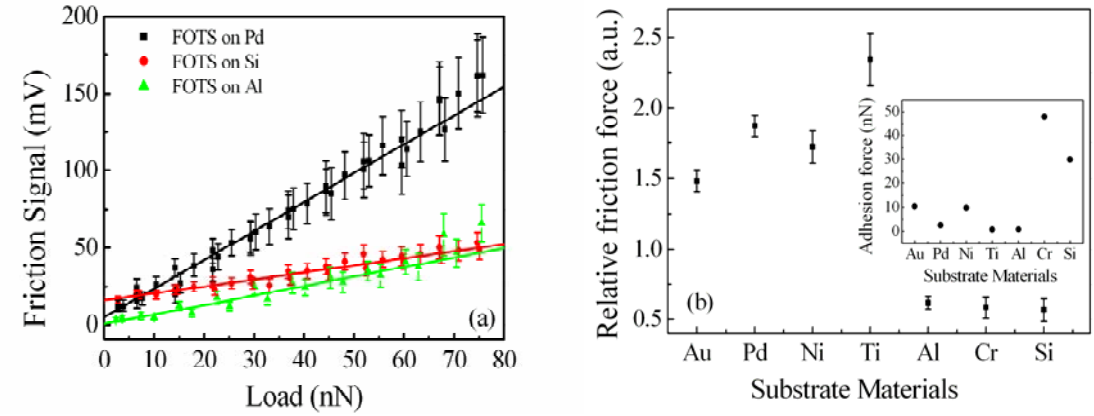

Figure 4 Friction signal vs. normal load applied by AFM tip (a), and the relative friction coefficient of FOTS on various substrates (b). The inset in (b) displays the adhesion force deduced from friction signals.

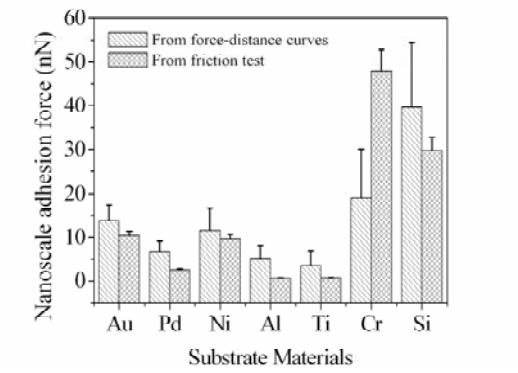

Figure 5. Comparison of the adhesive forces of FOTS on various substrates measured using force-distance curves and friction test in ambient air.

Figure 5 compares the adhesion forces between AFM tip and FOTS on various substrates measured by force-distance curves and friction test, respectively. The results measured by these two methods are in good agreement. The adhesion force between AFM tip and a surface is determined by the surface energy and the roughness of the surface. The competence of these two factors induces that the FOTS on Au, Pd, Ni, Al, and Ti has lower nano-scale adhesion force due to its larger roughness and FOTS on monocrystal silicon has largest nano-scale adhesion force.

4. Conclusions

$CF_3(CF_2)_5(CH_2)_2SiCl_3$ (FOTS) self-assembled monolayers have been grown on thin films of Au, Pd, Ni, Ti, Cr, and Al using a same process as that used for silicon substrates. The contact angle, surface energy, nano-scale adhesion force, and nano-scale friction behavior have been characterized. The metals can be ranked into two groups. One group has a behavior similar to silicon, for example, Ti, Al, and Cr. FOTS on those substrates displays an overall good anti-stiction performance, including high water contact angle, low surface energy, low adhesion and friction force. On the other hand, FOTS on other group of metals exhibit very low contact angle, high adhesion and friction force, indicating that FOTS molecule might be physically adsorbed onto those surface and have low coverage.

Acknowledgement

Financial support from Danish Research Council for Technology and Production Science is acknowledged, the Center of Individual Nanoparticle Functionality (CINF) is sponsored by the Danish National Research Foundation. Y X Zhuang would like to thank support from Northeastern Univeristy.

Reference

[1] Schreiber F 2000 *Prog. Surf. Sci.* **65** 151-256
[2] Baker M A and Li J 2006 *Surf. Interface Anal.* **38** 863-7
[3] Cox J D, Curry M S, Skirboll S K, Gourley P L and Sasaki D Y 2002 *Biomaterials* **23**: 929-35
[4] Lee N, Choi S and Kang S 2006 *Appl. Phys. Lett*. **88** 073101
[5] Zhuang Y X, Hansen O, Knieling T, Wang C, Rombach P, Lang W, Benecke W, Kehlenbeck M and Koblitz J 2006 *J. Micromech Microeng* **16** 2259-64
[6] Zhuang Y X, Hansen O, Knieling T, Wang C, Rombach P, Lang W, Benecke W, Kehlenbeck M and Koblitz J 2007 *J. Microelctromech. S.***16** 1451-60
[7] Mayer T M, de Boer M P, Shinn N D, Clews P J and Michalske T A 2000 *J. Vac. Sci. Technol. B* **18** 2433-39
[8] Ashurst W R, Carraro C and Maboudian R 2003 *IEEE Trans. Devices Mater. Reliab.* **3** 173-8
[9] Zhuang Y X and Menon A 2005 *J. Vac. Sci. Technol. A* **23** 434-9
[10] Liu H and Bhushan B 2003 *Ultramicroscopy* **97** 321-40
[11] Bhushan B and Liu H 2001 *Phys. Rev. B* **63** 245412